Evaluation of spectral radiative properties of gases in high-pressure combustion

Westlye, Fredrik R.; Hartz, Benjamin A.K.; Ivarsson, Anders; Fateev, Alexander; Clausen, Sønnik

Published in:
Journal of Quantitative Spectroscopy & Radiative Transfer

Link to article, DOI:
10.1016/j.jqsrt.2022.108089

Publication date:
2022

Document Version
Publisher's PDF, also known as Version of record

Journal of Quantitative Spectroscopy & Radiative Transfer 280 (2022) 108089

Contents lists available at ScienceDirect

Journal of Quantitative Spectroscopy & Radiative Transfer

journal homepage: www.elsevier.com/locate/jqsrt

Evaluation of spectral radiative properties of gases in high-pressure combustion

Fredrik R. Westlye[a,*], Benjamin A.K. Hartz[a], Anders Ivarsson[a,*], Alexander Fateev[b], Sønnik Clausen[b]

[a] Department of Mechanical Engineering, Technical University of Denmark, Nils Koppels Alle Bld. 403, 2800 Kgs. Lyngby, Denmark
[b] Department of Chemical Engineering, Technical University of Denmark, Frederiksborgvej 399, Bld. 313, DK-4000 Roskilde, Denmark

ARTICLE INFO

Article history:
Received 8 October 2021
Revised 21 January 2022
Accepted 21 January 2022
Available online 22 January 2022

Keywords:
CO_2
H_2O
FTIR spectroscopy
High temperature
High pressure
Correlated pseudo-Lorentzian line profile
Combustion

ABSTRACT

Radiative heat transfer affects local flame temperatures, and thus pollutant formation in high-pressure diffusion flames but the radiation properties of major gas species at pressures and temperatures relevant for combustion engines are not well known. In order to facilitate radiative transfer calculations in these types of flames, new and already published CO_2 and H_2O absorption spectra at high pressure and temperatures have been used to validate their modelled spectra based on the HITEMP 2010 database. Corrections for non-Lorentzian behavior of collisional-broadened lines have been evaluated, where an adjustable pseudo-Lorentzian line profile has been correlated for CO_2 – N_2 mixtures over a wide range of pressure, temperature and concentration. A fixed pseudo-Lorentzian line profile was found to give similar performance to previous empirical line corrections when comparing to available experimental H_2O data over a relatively wide pressure and temperature range. The work has led to the release of an in-house MATLAB code, named RadISpeC freely available for download. The code efficiently produces spectra for radiation calculations for both soot and gas at high pressures and temperature.

1. Introduction

Studies of radiation properties of gases at high pressure and temperature were initially related to the study of planetary atmospheres and emission from stars within the field of astronomy and astrophysics [1–3]. In the last few decades however, this topic has become increasingly important in studies of radiative heat transfer in various combustion applications. While the aim in other fields has been to understand and quantify the underlying physics related to discrepancies between modelled and measured spectra, such as e.g. the effect of line mixing, buffer gas, intermolecular bonding etc., the current work has a somewhat different ambition. The main goal of this work is to develop a modeling approach, which can be used for accurate and reliable prediction of gas radiation spectra at high pressures and temperatures. Gas radiation influences local temperature as it dissipates part of the energy released locally to the surroundings. Accurate calculations of local flame temperature and gas composition are crucial for predicting pollutant formation such as CO and NOx, as this process is largely temperature driven. Gas radiation calculations are notoriously difficult, time consuming and computationally expensive because they require spatial integration at each wavelength of high spectral resolution gas radiation spectra for each of the major gas components such as CO_2 and H_2O. Their radiation spectra are defined by local gas temperature variations and the individual emission spectra of CO_2 and H_2O at various pressures/temperatures are therefore required inputs to the calculations. In this context, experimental data of gas absorption at high pressure and temperature have started to emerge [4–8]. Experiments at pressures and temperatures relevant for combustion engines are however difficult to perform, and therefore the data available are sparse.

The present study aims to develop simplified spectral models suitable for use in calculations of radiative heat transfer, spectroscopic measurements and tomographic thermometry of high-pressure flames, particularly those occurring in compression ignition engines. These models consist of line-by-line radiation spectra calculations for major gaseous combustion products (CO_2 and H_2O) empirically modified to account for effects of high pressure and temperature.

2. Modeling of absorption by gases

IR-active molecules exhibit several (sometimes millions) narrow spectral lines associated with the ro-vibrational transitions of the

* Corresponding authors.
E-mail addresses: Fredrik.westlye@man-es.com (F.R. Westlye), ai@mek.dtu.dk (A. Ivarsson).

https://doi.org/10.1016/j.jqsrt.2022.108089
0022-4073/

specific molecule. Efforts have been made to map these transitions for molecules relevant to atmospheric and high-temperature applications. Spectral line databases for major species (H_2O, CO_2 and CO) have been developed (e.g. HITRAN, HITEMP, GEISA, BT2 and CDSD). These databases, based on a combination of available experimental data and theoretical calculations, can be used for modeling of high-resolution absorption/emission spectra of molecules at various temperatures and pressures. The HITRAN and the GEISA line lists have been developed to predict the spectral behavior of molecules at low to near room temperature [9,10], covering 39 and 22 gas molecules respectively, while HITEMP is a similar line list suitable for a range of high temperature applications [11]. The CDSD line lists are dedicated to CO_2 with more than 600 million transitions with hot transitions at temperatures as high as 4000 K [12]. Similarly, the BT2 list contains over 500 million transitions for the most common isotope of water $H_2^{16}O$ [13]. The line lists provide integrated intensities of isolated lines and lines center positions. In the HITRAN and HITEMP lists, the integrated spectral line intensities are conveniently given in $cm^{-1}/(molecule \bullet cm^{-2})$ at 296 K, and can be re-calculated to an auxiliary temperature T with use of Eq. (1).

$$S(T) = S_0 \frac{Q_0 \exp\left(-\frac{CE_0}{T}\right)\left(1-\exp\left(-\frac{C\nu_0}{T}\right)\right)}{Q \exp\left(-\frac{CE_0}{T_0}\right)\left(1-\exp\left(-\frac{C\nu_0}{T_0}\right)\right)} \quad (1)$$

Where the subscript 0 denotes reference conditions (1atm, 296 K), Q is the partition function evaluated with the TIPS database here [14], ν_0 is lines center, E_0 is lower state energy and C is a constant [15].

Spectral lines are not purely monochromatic; rather, the energy is distributed across a narrow spectral range because any process occurring over a finite amount of time has an intrinsic width in the frequency domain. The shape of the spectral lines depends on the nature of the transition, for which the damped oscillator model is the most widely accepted analogy, giving rise to the Lorentzian profile. The mechanism behind pressure broadening is that molecular collisions perturb the "damping", thus inducing a wider FWHM of the Lorentzian. Temperature broadening, also referred to as Doppler broadening, is a consequence of molecular motion relative to the observer, resulting in a Gaussian distribution about the line center. The combined effect of pressure and temperature is typically described with a Voigt line shape which is a convolution of the Lorentzian and Gaussian profiles.

Line specific broadening parameters used for calculations of single line profiles are included in the HITRAN and HITEMP line lists. These parameters are provided as γ_{air} and γ_{self} corresponding to air- and self-broadened, or resonance-broadening, half widths at 296 K, respectively. The half width γ_0 used in calculations, depends on the concentration, x, of the selected species as it takes air and self-broadening into account Eq. (2),

$$\gamma_0 = \gamma_{air}(1-x) + \gamma_{self}x \quad (2)$$

The collision-broadened half width, γ_c, is related γ_0 through Eq. (3).

$$\gamma_c = \gamma_0 \frac{p}{p_0}\left(\frac{T_0}{T}\right)^n \quad (3)$$

Where the exponent n is also line specific (when it is available).

However, at high-pressure the traditional approach to account for pressure broadening is insufficient and the present study seeks to improve simple empirical methods using the latest experimental high-pressure data. Presented calculations of absorption spectra is based on the HITEMP-2010 database [11] and performed using an in-house developed MATLAB code, RadISpeC. The code has been optimized for computational efficiency and is validated with the HITRAN application-programming interface (HAPI) [16]. RadISpeC is freely available for download from [17], where detailed documentation is also available. The RadISpeC code has following options for spectra calculation parameters: line intensity cut-off, line wings cut-off, basis line-shapes, pressure, temperature, spectral resolution and instrument line-shape function (ILS) as well as various shape corrections to the basis line-shapes. The basis line shape options include the Lorentzian, Voigt, Van Vleck-Weisskopf [18]and MT-CKD [19]. Since no analytical solution exists for the Voigt profile, it can be optionally calculated numerically with the use of either the Humlìček approximation [20] or the approximation given by Liu et. al. [21].

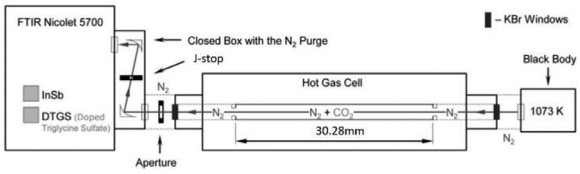

Fig. 1. Experimental set up with high-temperature flow gas cell.

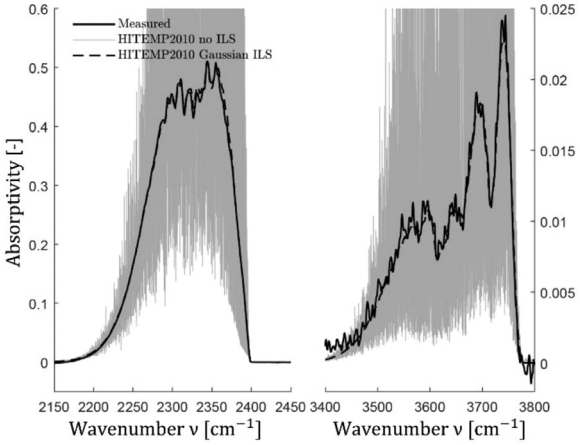

Fig. 2. Spectroscopic measurement of the 4.3 μm and 2.7 μm bands of CO_2 compared to spectra generated from HITEMP2010 assuming a pure Lorentzian line shape and convolved with the Blackman instrument line shape. The measurement is of 5% CO_2 in N_2 at 0.89 bar and 1000 K gas condition from [8] and this work.

2.1. CO_2

Available experimental data acquired at high pressures and temperatures have been used to validate the CO_2 spectra generated from HITEMP-2010 with various corrections to the line shapes applied. The majority of the data are from experiments conducted in the new high pressure and temperature gas cell at DTU [8] seen in Fig. 1.

CO_2 transmissivity spectra were acquired with a Nicolet 5700 high resolution FT-IR spectrometer and a gas cell with effective absorption path-length of 30.28 mm. An external IR light source was used in this setup and the spectral resolution was therefore defined by the optics collimating the beam (J-stop), entering the Michelson interferometer rather than the resolution specified by the FT-IR manufacturer. In addition, a Blackman apodization window was used to reduce spectral ringing. The optical resolution has been determined by fitting a calculated high-resolution HITEMP 2010 spectrum, convolved with the instrument line shape imposed by the Blackman window. Excellent agreement between measured data and HITEMP-2010 data is achieved (Fig. 2) with a spectral resolution of 2.2 cm^{-1} according to the Sparrow criterion [22]. At pressures from 20 atm and above, the broadened spectral lines become sufficiently wider than the ILS such that the FT-IR spectrometer is able to fully resolve the spectrum and therefore a correc-

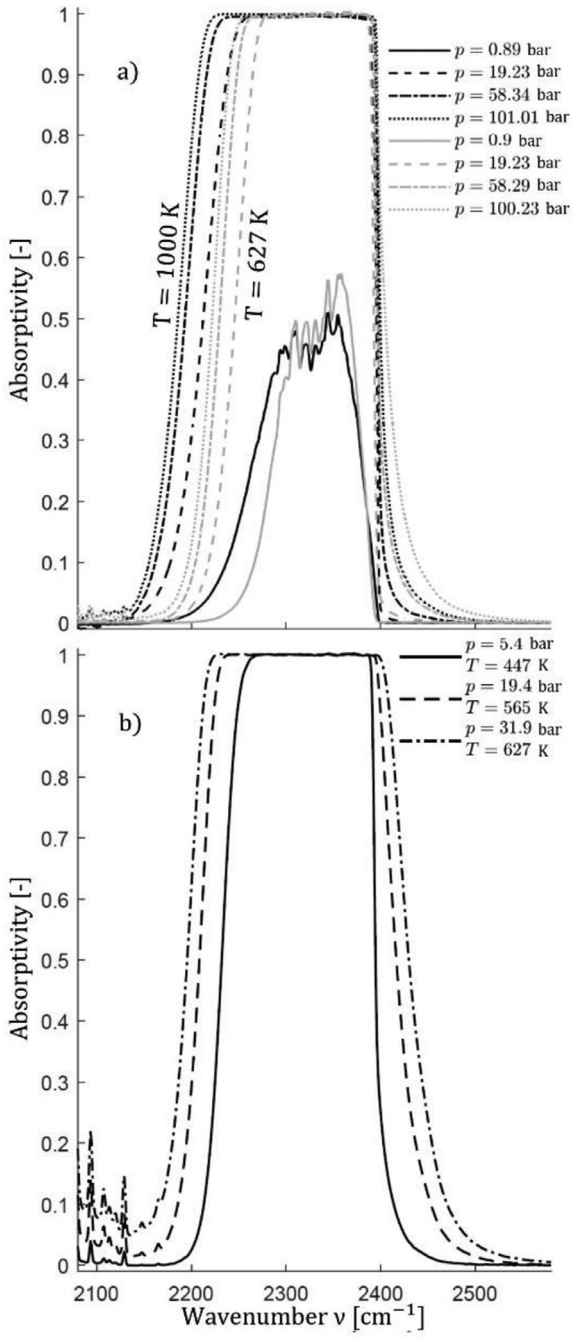

Fig. 3. Measured absorptivity, $(1\text{-}\tau)$, by the ν_3 band of CO_2 from [8] and this work. (a) 5% CO_2 in N_2 at 1000 K (black) and 627 K (gray) at pressures from 0.890 to 101 bar. (b) 100% CO_2 at three different conditions.

tion of the absorptivity spectrum to account for the ILS of the FTIR spectrometer is not necessary. In this case the measured spectrum is the true spectrum, i.e. not affected by the measurement instrument.

Measurements of 5% CO_2 in N_2 were made in a pressure range from 0.89 to 101.01 bar and at temperatures 627 and 1000 K. Also, measurements of 100% CO_2 at 5.41, 19.39 and 31.90 bar pressure and respective temperatures of 447, 565 and 627 K were made. The measured spectral absorption of CO2 is shown in Fig. 3.

The band head at 2397 cm^{-1} is apparent in the $CO_2 - N_2$ measurements at about 1 bar (Fig. 3(a)) with well-recognized slow decrease in absorptivity towards lower wavenumbers and relatively steep decrease at higher wavenumbers. At higher pressures, a more gradual absorptivity decay becomes increasingly apparent beyond the band head ($\nu > 2400$ cm^{-1}) and extends towards higher wavenumbers. This is a consequence of superposition of thousands of spectrally broadened lines within the band. The spectral region between 2400 to around 2600 cm^{-1} only consists of wing absorption from broadened lines. The shape of the absorptivity in this spectral region is a cumulative representation of the wings of pressure broadened lines and is thus an ideal basis for studying the average shape of these lines. It is apparent that absorptivity increases with molecular density, i. e. increases with pressure and decreases with temperature. The true effect of temperature and pressure are more intuitively visualized when translating the transmissivity spectra to the more general absorption cross-section spectra through Eq.(4).

$$\sigma = -\frac{\ln(\tau)RT}{Lx_{CO_2}pN_A} \tag{4}$$

The plateau region at the band top in Fig. 4 is not physical, but a consequence of the dynamic range of the FT-IR spectrometer. As one can see in Fig. 4 (a), pressure increases the cross-section beyond the band head in the 2400 -2600 cm^{-1} spectral range, while the P-branch (2150–2250 cm^{-1}) is not significantly affected. Temperature, on the other hand, widens the band due to an increase in thermal population of higher J-levels and hot bands. The thermal distribution only extends to lower wavenumbers due to the band head. At the same time, the cross-section reduces beyond the band head due to lower molecular density.

With 100% CO_2, the effect of pressure broadening can be seen in absorption cross-section spectra in Fig. 4 (b), when comparing the two band shapes from 5% and 100% CO_2 at 627 K (solid gray and solid black respectively). The band shapes nearly match in both the high and low wavenumber regions despite the 5% measurement having a significantly higher pressure. This implies that the broadening effect of resonance-, or self-broadening, is stronger than that of collision broadening. The shape of the continuum beyond the band head in Fig. 4 (b), gives the appearance that the wings of self-broadened lines decay differently compared to collision-broadened lines. The shape of the continuum from collision-broadened lines implies that single lines decay more rapidly from the line centers, while transitioning to a more gradual decay in the far wing compared to self-broadened lines. This behavior could be related to long lived dimer interactions [23].

Numerous studies of non-Lorentzian behavior of CO_2 absorption lines, primarily in the 4.3 μm band, exist [24,25,26,27,28,5]. Typically, true spectral lines have sub-Lorentzian wings and consequently super-Lorentzian line centers. A correction is required to account for non-Lorentzian behavior, especially for the 4.3 μm band of CO_2 due to the high intensity and density of the lines contained within the band.

Alberti et al. [29,30,31,32] have shown the error caused by the infinitely extended line wings of the full Lorentzian profile. They proposed band-shape correlations, based on experiments, describing a dynamic wing cut-off as function of pressure and temperature. The correction simply cuts off the wings of super-positioned Lorentzian lines at a specified wavenumber relative to γ_0. Consequently, this approach does not account for super-Lorentzian behavior near line centers and therefore does not conserve the integrated line intensity. For this reason, the correction is only applicable in an optical thickness range where the strong absorption lines are opaque and the far-wing contributions are negligible. Although the corrections of Alberti et al. are simple and efficient, large local deviations in the absorption coefficient may appear when broadening is severe. In addition, the cut-off imparts discontinuities in the spectra. The ensemble effect of which may distort the qualitative shape of vibrational bands.

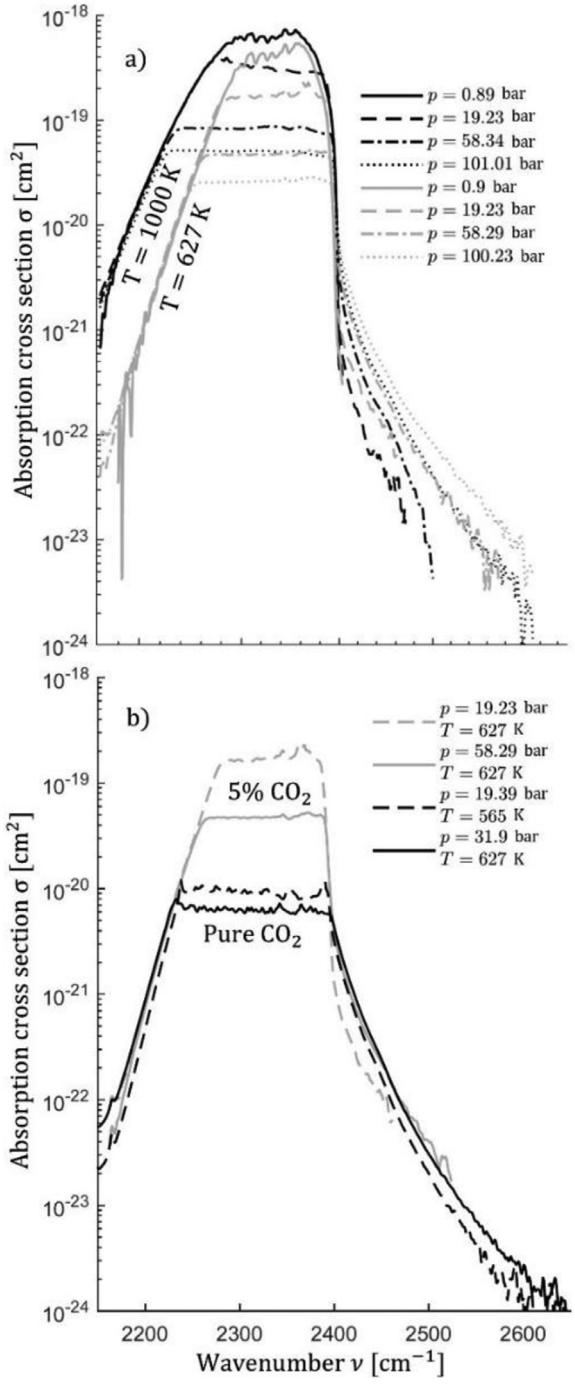

Fig. 4. (a) Measured absorption cross-section of 5% CO_2 in N_2 at 1000 K (black) and 627 K (gray) and a pressure range of 0.890–101 bar. (b) Measured absorption cross-section of 100%e CO_2 at three different conditions compared to 5% CO_2 in N_2 measurements at similar conditions.

Another correction approach frequently applied is the line wing correction, usually referred to as the χ-correction, where a correction coefficient between 0 and 1 is multiplied with the Lorentzian profile. The correction consists of exponentially decaying functions, each valid within a given spectral range from the line center, effectively suppressing the wings of the Lorentzian profile. This approach also has the drawback of not conserving the integrated line intensity and thus becomes inaccurate for dilute mixtures and low optical thickness as also demonstrated by Perrin & Hartmann [4]. Hartmann et al. [33] therefore proposed an additional correction,

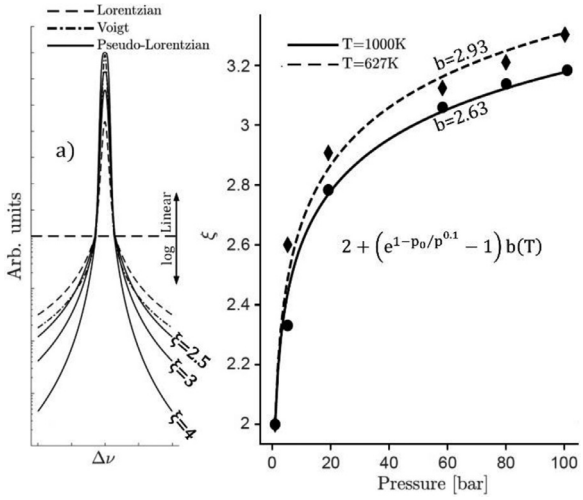

Fig. 5. a) The pseudo-Lorentzian profiles compared to the Lorentzian and the Voigt profile. The lower half of the y-axis is logarithmic while the upper half is linear in order to enhance the differences in both wings and peaks. b) The pressure dependency of the exponent ξ at 627 K and 1000 K fitted with the empirical expression $\xi = 2 + (e^{1-p_0/p^{0.1}} - 1)b(T)$.

where the entire line profile is multiplied by a density-dependent constant that compensates for the deviation from the integrated line intensity as consequence of the χ-correction. However, no correlation was developed for the approach, nor has it been applied in the literature. Perrin & Hartmann [5,4] examined line broadening at pressures approaching those in combustion engines, but only at a temperature range up to 800 K.

Instead of correcting the Lorentzian line profile, Price proposed a pseudo-Lorentzian profile [34]. The application was intended for Mössbauer spectroscopy, but the authors recognized its potential use in vibrational spectroscopy. A similar approach has been published earlier in a NASA report [35]. The profile has a single empirical parameter imposing sub-Lorentzian wings while conserving the integrated line intensity. The profile has the same formulation as the Lorentzian, only the wavenumber exponent, ξ, is set as a variable as seen in Eq. (5). Thus, for $\xi = 2$, the profile is simply the Lorentzian. The elegance of the profile is that it can be integrated analytically as shown in Eq. (6). This allows one to use the constant α to normalize the integral over the selected line. Examples of some pseudo-Lorentzian profiles compared to the Lorentzian and Voigt profiles can be seen in Fig. 5 (a).

$$L_p(\nu) = \frac{\alpha}{\left(1 + \left|\Delta\nu/\gamma_c\right|^{\xi}\right)} \tag{5}$$

$$\alpha = \frac{\xi \sin\left(\pi/\xi\right)}{2\pi\,\gamma_c} \tag{6}$$

The parameter ξ was determined by fitting simulated spectra to the measured spectra in the spectral range 2100–2600 cm^{-1} using a weighted least squares approach. In this approach, the residuals are weighted with τ^2 to account for the variance of noise in the spectroscopic measurements [36]. This ensures that the saturated spectral region does not affect the quality of the fit.

The fitted ξ values and the resulting spectra can be seen in Figs. 5 (b) and 6 respectively. Fig. 6 also shows that the χ-correction by Perrin & Hartmann gives a good approximation to the continuum in the experimental data. The ξ fit has been pressure and temperature correlated with the empirical function in Eq. (7).

$$\xi(p, T) = 2 + \left(e^{1-p_0/p^{0.1}} - 1\right) b(T) \tag{7}$$

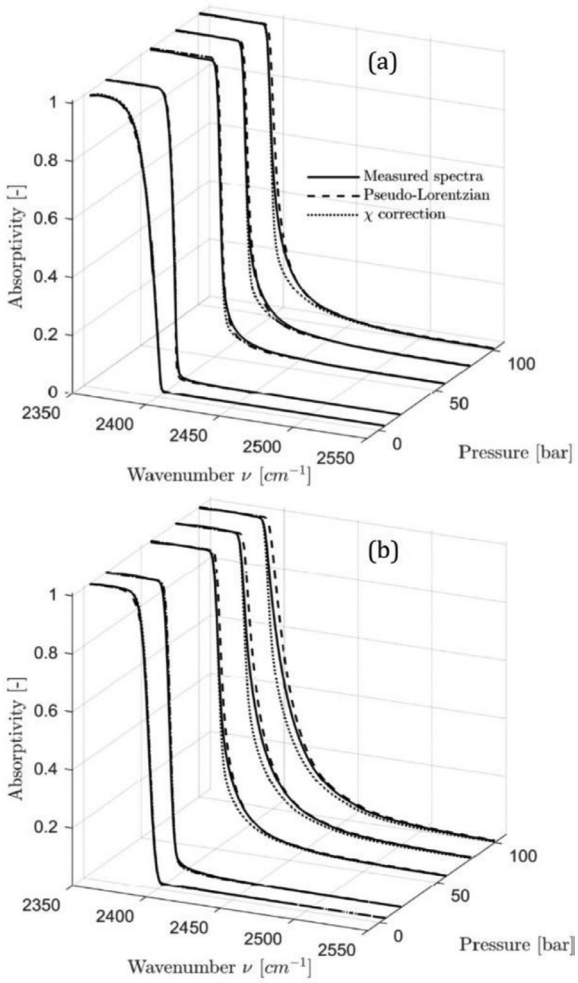

Fig. 6. Modelled spectra of the ν_3 continuum of CO_2 using (– – –) the fitted pseudo-Lorentzian from present work and (• • • • • • • • •) the χ-correction by Perrin & Hartmann [4] compared to (-) measurements of 5% CO_2 in N_2 at (a) 1000 K and (b) 627 K in pressure range of 0.9–100 bar.

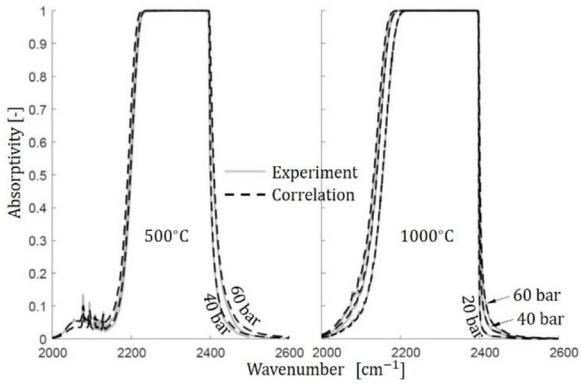

Fig. 7. Modelled spectra using the pseudo-Lorentzian with the correlation for ξ in Eq. (8) is shown in dashed lines compared to measurements of 20% CO_2 in N_2 shown in gray.

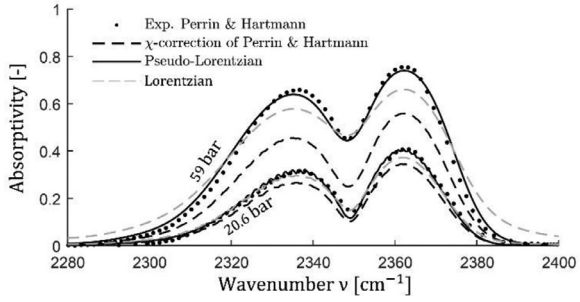

Fig. 8. Modelled spectra of the 4.3 μm band of CO_2 using a pseudo-Lorentzian profile with ξ based on Eq. (7) with b =3.66(-), the χ-correction by Perrin & Hartmann (– – –) and the Lorentzian (– – –). Experimental data by Perrin & Hartmann [4] of 88 ppm CO_2 in N_2 at 296 K and elevated pressure of 20.6 and 59 bar in a 4.4 cm cell (•).

Where p_0 is a reference pressure of 1atm, p is the total pressure in atm and b(T) is a function of temperature. Effects of concentration were difficult to discern as the dataset only consisted of 5 % and 100 % CO_2.

One can expect the function b(T) to be inversely related to temperature due to the inverse relation to γ_c,Eq. (3). Assuming that b(T) takes on the form $x_1(\frac{T_0}{T})^{x_2}$, one can calculate x_1 and x_2 using the fitted b values shown in Fig. 5 (b) by solving $x_1 = \frac{2.93}{(296/627)^{x_2}} = 3.48$ and $x_2 = \ln(\frac{2.63}{2.93})/\ln(\frac{627}{1000}) = 0.23$ from the data fit of 627 K and 1000 K measurements shown in Fig. 6.

This correlation has been tested against newly acquired measurements of 20 % CO_2 in N_2 at 773 K at 40 and 60 bar, and 1273 K at 20, 40 and 60 bar. It was found that the correlation performs excellently when factoring in the concentration of CO_2 as shown in Eq. (8).

$$\xi(p,T) = 2 + a(p)b(T)(1 - x_{CO_2}) \tag{8}$$

Where $a(p) = (e^{1-p_0/p^{0.1}} - 1)$ and $b(T) = 3.66(T_0/T)^{0.23}$. Notice that x_1 in b(T) becomes 3.66 when accounting for the CO_2 concentration of 5 % in the measurements of which the correlation was based. The performance of the correlation in modeling the spectra at 500 and 1000 °C can be seen in Fig. 7.

At pressures from atmospheric and below, the pure Lorentzian (i. e. $\xi = 2$) is assumed to give the best fit. Thus, Eq. (8) is only valid for p > 1 bar. However, due to the steep gradient in ξ from 1–5 bar and the lack of measurements in this pressure range, the correlation is considered applicable in the pressure range 5–100 bar. The correlation in Eq. (8) also produces a good fit to the dilute low temperature measurements at 296 K taken from [4]. The conservation of integrated line intensity makes the pseudo-Lorentzian profile more accurate under optically thin conditions compared to the χ-correction approach as demonstrated in Fig. 8. The pseudo-Lorentzian predicts the band centers well despite the fact that the ξ was fitted from the spectra of less dilute CO_2 at higher temperature.

The concentration dependence in Eq. (8) results in a Lorentzian profile for 100 % CO_2, which does not match the measurements well. The correlation is therefore limited to the concentration range up to 20% CO_2 for which it is so far validated. However, it should be emphasized that the concentration range from 0–20% CO_2 covers the majority of practical spectroscopy of flames. Nevertheless, the performance of the pseudo-Lorenztian approach for self-broadened lines has been investigated. The profile (Eq. (5)) does not appear able to mimic the basic shape of the line profile of self-broadened lines as well as collision-broadened lines, as seen in Fig. 9 a). Indeed, it is apparent that the line shape changes when self-broadening dominates as also observed in Fig. 4 (b).

The impact of sub-Lorentzian correction on radiative heat transfer may be somewhat elusive to quantify, as it depends on the molecular density and path length of the specific case. This is evident in Fig. 4, where higher molecular density reveals lower cross-sections and saturate the higher cross-sections that fall within the dynamic range of the spectrometer. The absorption cross-sections shown in Fig. 10 is thus an intuitive way of illustrating the im-

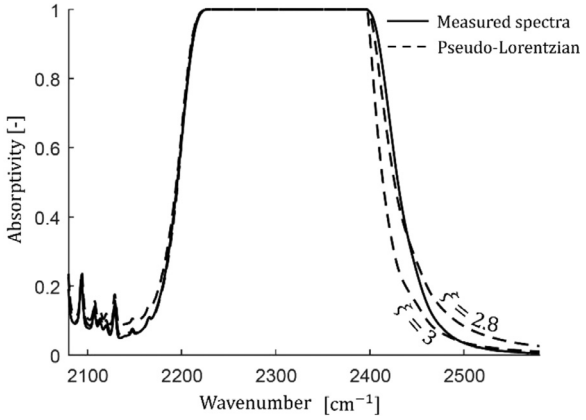

Fig. 9. Pseudo-Lorentzian with two different values of ξ ($- - -$) compared to measurement of Pure CO_2 at 39.1 bar and 627 K (-).

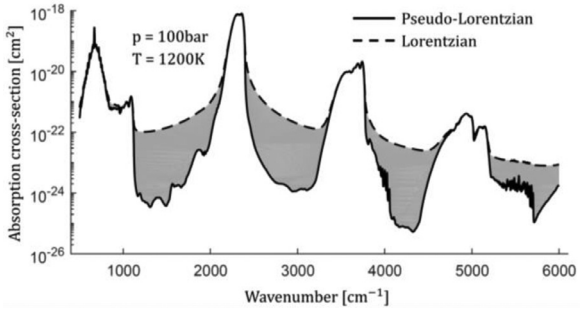

Fig. 10. Modelled absorption cross-section of 5 % CO_2 in N_2 at 100 bar and 1200 K using a Lorentzian profile (dashed line) and the correlated pseudo-Lorentzian profile (solid line).

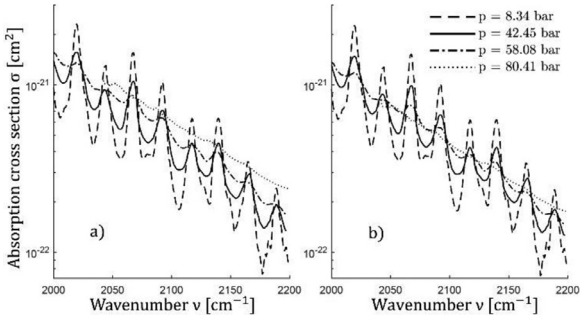

Fig. 11. Transmissivity measurements from Hartmann et al. [6] converted to absorption cross-section assuming (a) ideal gas behavior and (b) real gas behavior. The measurements are of the ν_2 band wing of pure H_2O at 575 K and a range of pressures.

pact of the pseudo-Lorentzian correction. One can deduct that the difference between calculated radiative heat transfer using the Lorentzian and Pseudo-Lorentzian increases with molecular density and optical path length.

In optical diagnostics, it may have significant impact that N_2 broadened CO_2 lines at concentrations up to 20 % over a wide range of pressures and temperatures can be well predicted with the use of the pseudo-Lorentzian line profile. The accurate prediction of the 4.3 μm band shape makes the correlated Pseudo-Lorentzian attractive for use in spectral based thermometry of high-pressure flames, utilizing the thermal- and pressure broadening as additional inputs for the tomographic reconstruction of local temperatures in axis-symmetrical flames. In addition, the conservation of the integrated line intensity makes the profile versatile with respect to optical thickness, an important property for modeling of radiative transfer with steep gradients in temperature and gas concentrations. In these cases, the developed pseudo-Lorentzian approach gives a simple and flexible line-shape modeling tool for CO2 emission spectra modeling.

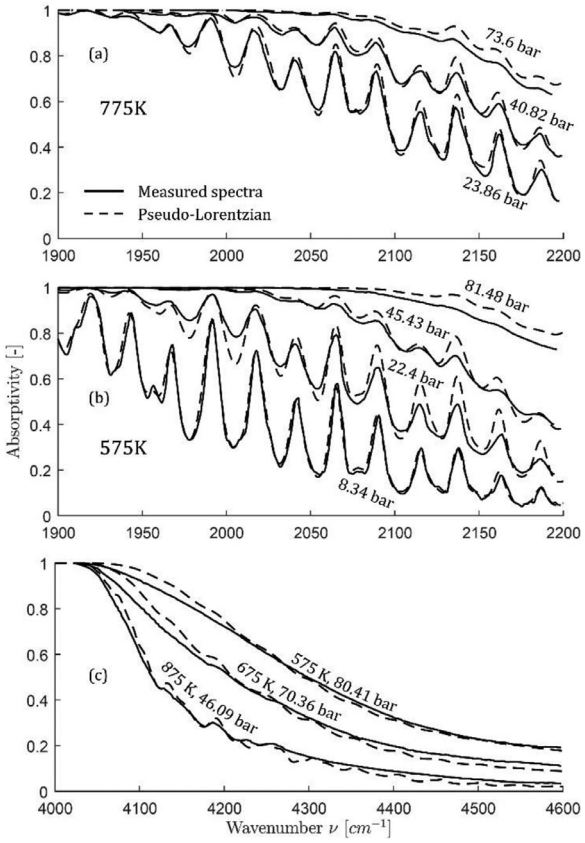

Fig. 12. H_2O spectra modeled using the pseudo-Lorentzian line shape with $\xi = 2.4$ ($- - -$) compared to measurements from Hartmann et al. [6] of the ν_2 band at (a) 575 K and (b) 775 K and (c) the (ν_1,$2\nu_2$,ν_3) triad at 3 different densities.

It should be mentioned that foreign-broadening of CO_2 lines by H_2O, and vice versa, are important in the context of hydrocarbon flames. Such interaction was also recognized by Perrin & Hartmann, who investigated the H_2O-broadening of CO_2 lines at high temperatures, but at sub atmospheric pressures [37]. Later studies have shown that H_2O has an impact on CO_2 [38–42] broadening in CO_2 + H_2O mixtures. Unfortunately, such measurements at elevated pressure and temperatures are very limited and must be subject for further work.

2.2. H_2O

The H_2O absorption continuum is an extensively studied topic in the environmental science. The majority of these studies are thus concerning sub-atmospheric to atmospheric pressure and low temperatures [43–45], while literature regarding H_2O line broadening at elevated temperatures and pressures is limited. Thomas [7] and Hartmann et al. [6] are probably the most cited works in this regard.

The polarity of H_2O makes it more susceptible to dimerization which may induce shifts in spectral peaks, broaden the lines and add certain broadband spectral features affecting the continuum [46]. Such effects are not accounted for in the spectral molecular databases, making H_2O difficult to model. However, dimerization is less significant at the temperatures, concentrations and pressures relevant to flames.

Several of the measurements by Hartmann et al. [6] were made under conditions near saturation where dimerization is significant. They used the modified Berthelot equation of state to account for

real gas effects on the molecular density. The molecular density may alternatively be corrected by using an effective path length, $L' = L/Z$, where Z is the compressibility factor found with a real gas equation of state. The real gas behavior is evident when converting transmissivity to cross-section using Eq. (4) as seen in Fig. 11 (a). The cross-section is significantly overestimated when assuming ideal gas, especially near saturated conditions. Replacing L with L' in Eq. (4) corrects for the deviations from ideal gas, isolating the effects of broadening as seen in Fig. 11 (b).

Hartmann et al. [6] developed a χ- based correction for modeling spectra of pure water over a wide pressure and temperature range in two narrow spectral ranges of the ν_2 band wing (1900–2600 cm^{-1}) and the ($\nu_1, 2\nu_2, \nu_3$) triad wing (3900–4600 cm^{-1}). With a constant value of $\xi = 2.4$, the pseudo-Lorentzian profile was found to provide similar performance as the χ-correction of Hartmann when comparing to measurements in the ν_2 band as well as the (ν_1,$2\nu_2$,ν_3) triad over a wide range of temperatures and pressures as seen in Fig. 12.

It should be emphasized that the measurements here are of pure water vapor which is not relevant to combustion applications. Nevertheless, the results indicate that the pseudo-Lorentzian can be used as an empirical line shape for H_2O as well as CO_2.

3. Conclusion

Detailed analysis of the spectral properties of major combustion products such as CO_2 and H_2O have been performed to facilitate experimental and modeling investigations of radiative heat transfer in high-pressure flames. At pressures relevant for practical combustion applications, line corrections to account for deviations from Lorentzian/Voigt profiles are important, especially for CO_2 due to the dense-packed strong lines in the ν_3 band. Parameters and corrections applied to calculate molecular spectra have been rigorously validated against measurements. Some previously reported empirical corrections have been investigated and further development have been made of an empirical pseudo-Lorentzian line profile approach, previously applied in Mössbauer spectroscopy. This approach offers simplicity over previously published far wing χ-corrections, with its single fitting parameter ξ. In addition, it maintains the integrated line intensity and is thus applicable for high as well as low optical thicknesses.

The pseudo-Lorentzian is excellent in recreating the qualitative band shape in the modelled spectra compared to the experimental data of $N_2 + CO_2$ mixtures. A correlation for ξ has thus been established for $N_2 + CO_2$ mixtures over a wide pressure, temperature and concentration range. The correlation performs well when tested against newly acquired high temperature and pressure spectra of 20% CO_2 − 80% N_2.

The dipole interaction occurring in self-broadened lines appears to impose a different line shape than collision-broadened lines. This observation is made on the appearance of the band shape of pure CO_2 compared to $N_2 + CO_2$, and the fact that the pseudo-Lorentzian is unable to reproduce the shape of the absorptivity continuum beyond the band head. The correlation is thus limited to the concentration range investigated here.

It was found that a value of $\xi = 2.4$ gives similar performance to the previously proposed empirical line correction for pure H_2O, indicating the potential for the use of the pseudo-Lorentzian in dilute H_2O mixtures relevant to combustion.

4. Author statement

4.1. Copyright assignment

The undersigned authors transfer all copyright ownership of this manuscript to Journal of Quantitative Spectroscopy and Radiative Transfer, in the event the work is published. The undersigned authors warrant the article is original, does not infringe upon any copyright or other proprietary right of any third party, is not under consideration for publication by any other journal, and has not been published previously. The authors confirm that they have reviewed and approved the final version of the manuscript.

Declaration of Competing Interest

We hereby confirm that there are no known conflicts of interest associated with the publication " Evaluation of spectral radiative properties of gases in high-pressure combustion" and that none of the financial support for this work has had any influence on its outcome.

Sincerely,
Fredrik Ree Westlye

Acknowledgments

The authors would like to acknowledge the Danish Strategic Research Council (DSF), Technical University of Denmark - Department of Mechanical Engineering (DTU-Mech); Danish Maritime Fund; Orient's Fund; Lauritzen Fonden; The TORM Foundation; A.P. Moller and Chastine Mc-Kinney Moller's Fund for funding this work. This project has also partly received funding from the EMPIR program co-financed by the Participating States and from the European Union's Horizon 2020 research and innovation program (Grant number 17IND07 DynPT).

Reference

[1] Young LDG. High resolution spectra of venus. Icarus 1972;17:632–58.
[2] Connes P, Michel G. Astronomical fourier spectrometer. Appl Opt 1975;14(9):2067.
[3] Connes P, Michel G. High-resolution spectra of stars and planets. Astrophys J 1974;190:29–32.
[4] Perrin MY, Hartmann JM. Temperature-dependent measurements and modelling of absorption by CO2-N2 mixtures in the far line-wings of the 4.3micron CO2 band. J Quant Spectrosc Radiat Transfer 1989;42(4):311–17.
[5] Hartmann JM, Perrin MY. Measurements of pure CO2 absorption beyond the v3 bandhead at high temperature. Appl Opt 1989;28(13):2550–3.
[6] Hartmann JM, Perrin MY, Ma Q, Tipping RH. The infrared continuum of pure water vapor: calculations and high-temperature measurements. J Quant Spectrosc Radiat Transfer 1993;49(6):675–91.
[7] Thomas ME. Infrared- and millimeter-wavelength continuum absorption in the atmospheric windows: measurements and models. J Infrared Phys 1990;30(2):161–74.
[8] Christiansen C, Stolberg-Rohr T, Fateev A, Clausen S. High temperature and high pressure gas cell for quantitative spectroscopic measurements. J Quant Spectrosc Radiat Transfer 2016;169:96–103.
[9] Rothman LS, Gordon IE, Babikov Y, Barbe A, Benner DC, et al. The HITRAN2012 molecular spectroscopic database. J Quant Spectrosc Radiat Transfer 2013;130:4–50.
[10] Jacquinet-Husson N, Scott NA, Chédin A, Crépeau L, Armante R. The GEISA spectroscopic database: current and future archive for Earth and planetary atmosphere studies. J Quant Spectrosc Radiat Transfer 2008;109:1043–59.
[11] Rothman LS, Gordon IE, Barber RJ, Dothe H, Gamacje RR, Goldman A, Perevalov VI, Tashkun SA, Tennyson J. HITEMP, the high-temperature molecular spectroscopic database. J Quant Spectrosc Radiat Transfer 2010;111:2139–50.
[12] Taskun SA, Perevalov VI. CDSD-4000: High-resolution, high-temperature carbon dioxide spectroscopic databank. J Quant Spectrosc Radiat Transfer 2011;112(9):1403–10.
[13] Barber RJ, Tennyson J, Harris GJ, Tolchenov RN. A high accuracy computed water line list. Month Notice Roy Astron Soc 2006;368:1087–94.
[14] Laraia AL, Gamache RR, Lamouroux J, Gordon IE, Rothman LS. Total internal partition sums to support planetary remote sensing. Icarus 2011;215:391–400.
[15] Rothman LS, Rinsland CP, Goldman A, Massie ST, Edwards DP, Flaud J-M, Perrin A, Camy-Peyret C, Dana V, Mandin J-Y, Schroeder J, McCann A, Gamache RR, Watson RB, Yoshino K, Chance KV, Varnasi P. THE Hitran molecular spectroscopic database and hawks (Hitran atmospheric workstation): 1996 edition. J Quant Spectrosc Radiat Transfer 1998;60(5):665–710.
[16] Kochanov RV, Gordon IE, Rothman LS, Wcislo P, Hill C, Wilzewski JS. HITRAN Application Programming Interface (HAPI): A comprehensive approach to working with spectroscopic data. J. of Quantitative Spectroscopy & Radiative Transfer 2016;177:15–30.

[17] B.A.K. Hartz, "RadlSpeC program code (.m files and GUI for Matlab IDE), DOI: 10.6084/m9.figshare.6988997.v8," 2021.
[18] Van Vleck JH, Weisskopf VF. On the shape of collision-broadened lines. Rev Mod Phys 1945;17(227).
[19] Mlawer EJ, Payne VH, Moncet J-L, Delamere JS, Alvarado MJ, Tobin DC. Development and recent evaluation of the MT-CKD model of continuum absorption. Philos Transact A Math Phys Eng Sci 2012;370:2520–56.
[20] Humlìček J. Optimized computation of the Voigt and complex probability functions. J Quant Spectrosc Radiat Transfer 1982;27(4):437–44.
[21] Liu Y, Lin J, Huang G, Guo Y, Duan C. Simple empirical analytical approximation to the Voigt profile. J Opt Soc Am B 2001;18(5):666–72.
[22] Sparrow CM. On spectroscopic resolving power. Astrophys J 1916;44:76–87.
[23] Afsin RE, Buldyreva JV, Sinyakova TN, Oparin DV. Communicaiton: evidence of stable van der Waals CO2 clusters relevant to venus atmosphere conditions. J Chem Phys 2015;142:051101.
[24] Winters BH, Silverman S, Benedict WS. Lineshape in the wing beyond the band head of the 4.3 μm band of CO2. J Quant Spectrosc Radiat Transfer 1964;4:527–37.
[25] Burch DE, Gryvnak DA, Patty RR, Bartky CE. Absorption of infrared radiant energy by CO2 and H2O. IV. Shapes of collision-broadened CO2 lines*. J Opt Soc Amer B Opt Phys 1969;59(3):267–80.
[26] Le Doucen R, Cousin C, Boulet C, Henry A. Temperature dependence of the absorption in the region beyond the 4.3 μm band head of CO2. 1: Pure CO2 case. Appl Opt 1985;24(6):897–906.
[27] Cann MWP, Nicholls RW, Roney PL, Blanchard A, Findlay FD. Spectral line shape for carbon dioxide in the 4.3-micron band. Appl Opt 1985;24(9):1374–84.
[28] Cousin C, Le Doucen R, Boulet C, Henry A. Temperature dependence of the absorption in the region beyond the 4.3-micron band head of CO2. 2: N2 and O2 broadening. Appl Opt 1985;24(22):3899–907.
[29] Alberti M, Weber R, Mancini M. *Re*-creating Hottelś emissivity charts for carbon dioxide and extending them to 40 bar pressure using HITEMP-2010 data base. Combust Flame 2015;162:597–612.
[30] Alberti M, Weber R, Mancini M. *Re*-creating Hottel's emissivity charts for water vapor and extending them to 40 bar pressure using HITEMP 2010 data base. Combust Flame 2016;169:141–53.
[31] Alberti M, Weber R, Mancini M. Absorption of infrared radiation by carbon monoxide at elevated temperatures and pressures: Part A. Advancing the line-by-line procedure based on HITEMP-2010. J Quant Spectrosc Radiat Transfer 2017;200:258–71.
[32] Alberti M, Weber R, Mancini M, Fateev A, Clausen S. Validation of HITEMP-2012 for carbon dioxide and water vapour at high temperatures and atmospheric pressures in 450-7600 cm-1 spectral range. J Quant Spectrosc Radiat Transfer 2015;157:14–33.
[33] Hartmann JM, Bouanich JP, Boulet C, Sergent M. Absorption of radiation by gases from low to high pressures. I. Empirical line-by-line and narrow-band statistical models. J Phys II 1991;1:739–62.
[34] Price DC. Empirical lineshape for computer fitting of spectral data. Aust J Phys 1981;34:51–6.
[35] Ludwig CB. Study on exhaust plume radiation predicitons. NASA-George C Marshall Space Flight Center, Huntsville; 1968.
[36] Haaland DM, Easterling RG. Application of New Least-squares Methods for quantitative infrared analysis of multicomponent samples. Appl Spectrosc 1982;36(6):665–73.
[37] HartmannJ. M. Rosemann L, Perrin MY, Taine J. Diode-laser measurements and calculations of CO2-line broadening by H2O from 416 to 805 K and by N2 from 296 to 803 K. J Quant Spectrosc Radiat Transfer 1988;40(5):569–76.
[38] Sung K, Brown LR, Teth RA, Crwaford TJ. Fourier transform infrared spectroscopy measurements of H2O-broadened half-widths of CO2 at 4.3 μm. Can J Phys 2009;87:469–84.
[39] Wallace CJ, Jeon C, Anderson CN, Havey DK. H2O broadening of a CO2 line and its nearest neighbours near 6360 cm-1. J Phys Chem A 2011;115:13804–10.
[40] Delahaye T, Landsheere E, Pangui E, Huet F, Hartmann JM, Tran H. Broadening of CO2 lines in the 4.3 μm region by H2O. J Mol Spectrosc 2016;326:17–20.
[41] Tran H, Turbet M, Chelin P, Landsheere X. Measurements and modeling of absorption by CO2 + H2O mixtures in the spectral region beyond the CO2 $\nu 3$ -band head. Icarus 2018;306:116–21.
[42] Baranov YI. On the significant enhancement of the continuum-collision induced absorption in H2O+CO2 mixtures. J Quant Spectrosc Radiat Transfer 2016;175:100–6.
[43] Clough SA, Kneizys FX, Davies RW. Line shape and water vapor continuum. Atmos Res 1989;23:229–41.
[44] Clough SA, Iacono MJ, Moncet JL. Line-by-line calculation of atmospheric fluxes and cooling rates: Application to water vapor. J Geophys Res 1992;97:15761–85.
[45] Burch DE, Alt RL. Continuum absorption by H2O in the 700-1200 cm-1 and 2400-2800cm-1 windows. Air Force Geophysical Laboratory, Hasncom AFB, MA; 1984.
[46] Mukhopadhyay A, Cole WTS, Saykally S. The water dimes I: Experimental characterization. Chem Phys Lett 2015;633:13–26.